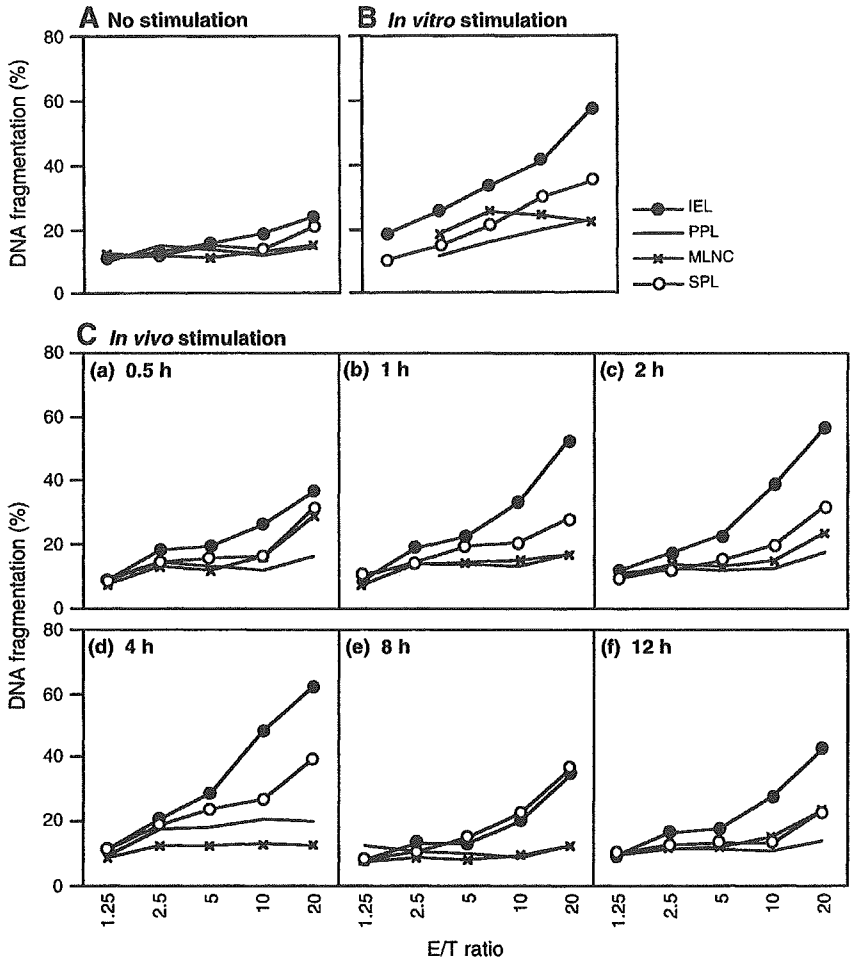

Fig. 5. Fas-mediated killer activity of lymphocytes. Lymphocytes isolated from naive C3H/HeN mice were cultured in the absence (A) or presence (B) of plate-bound anti-CD3 antibody. (C) Lymphocytes isolated from anti-CD3-injected C3H/HeN mice at different times after treatment were cultured in the absence of anti-CD3 antibody. Lymphocytes were pooled from three mice and a representative experiment of two performed is shown. The percentage of DNA fragmentation of Jurkat cells was measured and calculated as described in *Fas-mediated cytotoxicity assay* in Methods.

naive mice and increased at 4 and 24 h after the antibody injection. The number of $CD3^+$ cells and the density of CD3 expression on both IEL and SPL decreased at 4 h due to down-regulation of CD3, as previously reported (28–30). However, these values recovered by 24 h after the injection. Conversely, the amount of the activation marker, CD69, on both IEL and SPL was increased at 4 h after the injection and decreased to normal levels at 24 h, suggesting a rapid, temporary T cell activation.

Thymus-derived lymphocytes are involved in both phases of IEC apoptosis induced by anti-CD3

To directly confirm the involvement of thymus-derived T cells in the apoptosis observed here, we injected anti-CD3 into nude mice (Fig. 7). In euthymic BALB/c, the antibody induced bi-phasic apoptosis similar to that observed in C3H/HeN. By contrast, in athymic nude mice, both phases of apoptosis were almost completely abrogated, being depressed to the same levels as observed in normal BALB/c that were not administered antibody.

Adoptive transfer reconstitutes IEC apoptosis in nude mice

These data suggested the following hypotheses: the first phase of apoptosis at 4 h after the injection was induced by thymus-derived IEL, and the second phase at 24 h was induced by peripheral lymphocytes. To test these hypotheses, we adoptively transferred SPL or IEL isolated from euthymic mice into nude mice at 1 day before the anti-CD3 injection (Fig. 8, experiment 1). Transfer of SPL followed by anti-CD3 resulted in a substantial reconstitution of the second phase of apoptosis with crypt hyperplasia without villous apoptosis/destruction (Fig. 8, experiment 1B). However, neither phase of apoptosis was induced by the antibody in mice into which IEL had been transferred (Fig. 8, experiment 1). In addition, we adoptively transferred SPL and IEL successively, then administered anti-CD3. Unexpectedly, dual grafting of SPL

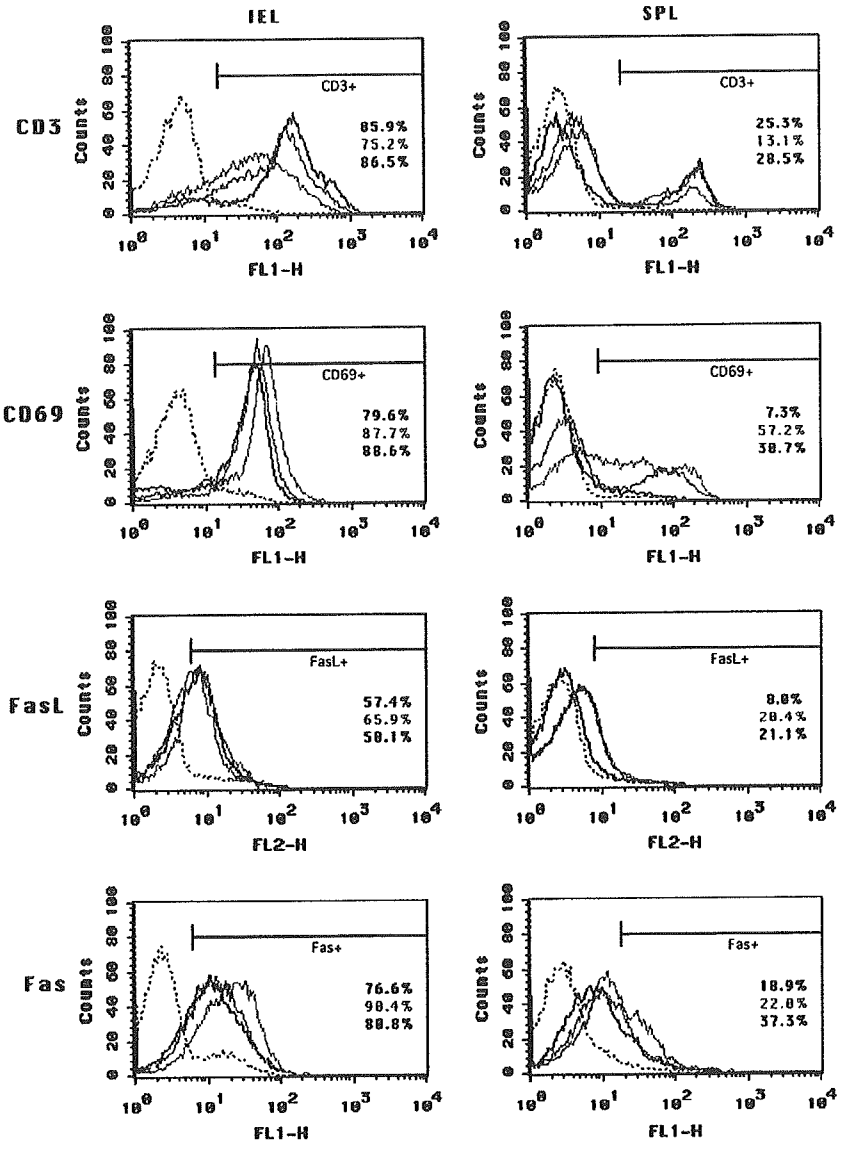

Fig. 6. Expression of CD3, CD69, FasL and Fas on IEL and SPL. Lymphocytes were isolated from naive (black line) or anti-CD3-treated C3H/HeN mice 4 (red line) and 24 (blue line) h after the injection and pooled from three mice. A representative experiment of the three performed is shown. The dotted line represents the isotype control. Numbers indicate the percentages of positive cells.

and IEL from euthymic mice induces neither the first phase nor the second phase of apoptosis in nude mice (Fig. 8, experiment 1B).

In experiment 2, because the migration of transferred IEL into the intestinal epithelium has been reported to take more than several weeks (31, 32), we changed the timing of IEL transfer. We adoptively transferred IEL, and after 5 weeks, the anti-CD3 antibody was injected (Fig. 8, experiment 2). IEL transfer significantly induced not only the first phase of apoptosis at 4 h (Fig. 8, experiment 2A) but also the second phase of apoptosis at 24 h after the anti-CD3 injection (Fig. 8, experiment 2B). Further, substantial apoptosis was detected in the villus at 24 h, which had not been so prominent in anti-CD3 antibody-treated euthymic BALB/c mice. Finally, differing from the results of experiment 1, dual grafting of SPL and IEL showed additive effects on IEC apoptosis (Fig. 8, experiment 2).

In the transfer experiments without anti-CD3 injection, no aberrant morphological changes were observed and no aberrant IEC apoptosis occurred following adoptive transfer of IEL, SPL or both (data not shown).

Discussion

In the present study, the following results were obtained: (i) anti-CD3 injections induced the apoptosis of small intestinal IEC bi-phasically with different spatial and temporal patterns,

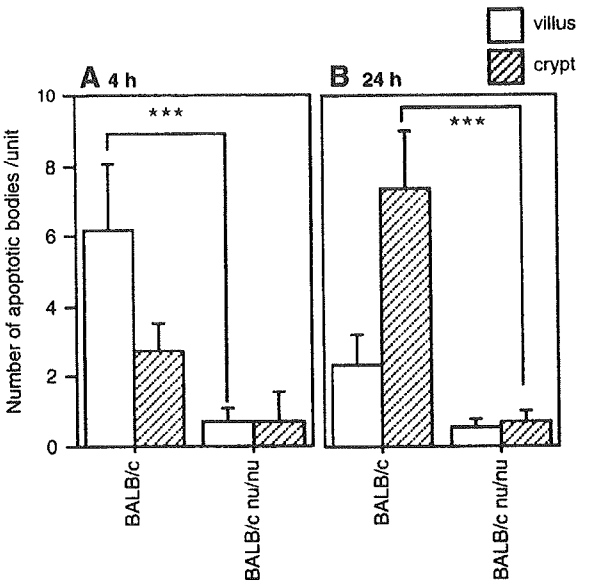

Fig. 7. Differences between the number of apoptotic cells in BALB/c and BALB/c *nu/nu* mice after intraperitoneal anti-CD3 (12.5 μg per mouse) administration. Apoptotic bodies with clearly fragmented and/or condensed nuclei, the most classical and definitive feature of apoptosis, were counted as described in Methods. Data represent the means ± SD of apoptotic cells per villus per crypt unit 4 (A) and 24 h (B) after antibody administration (number of mice = 4). The number of apoptotic bodies in mice administered with saline instead of anti-CD3 was <1.5 for both strains. The experiment was repeated three times with similar results. ***$P < 0.0005$.

(ii) each phase of apoptosis depended on Fas/FasL, (iii) anti-CD3 induced Fas-dependent cytotoxicity mediated by IEL rapidly, and by SPL gradually, (iv) each phase of apoptosis depended on thymus-derived T cells, (v) the adoptive transfer of SPL from euthymic mice to nude mice reconstituted only the second phase of IEC apoptosis, (vi) the adoptive transfer of IEL reconstituted both phases of IEC apoptosis, when anti-CD3 antibody was administered at 5 weeks after IEL transfer and (vii) dual grafting of SPL and IEL showed either abrogative or additive effects on IEC apoptosis, depending on the engrafting protocol.

A few studies have characterized the pathology and pathogenesis of anti-CD3 antibody-induced small intestinal lesions (33, 34). Merger *et al.* (17) demonstrated that multiple pathways of cytotoxicity, including tumor necrosis factor-α (TNF-α)-, Fas/FasL-, and perforin-mediated apoptosis, were associated with architectural damage. We have employed a model of enteropathy induced by a protocol similar to theirs, but some different results were obtained. Our data demonstrated that the antibody-induced bi-phasic apoptosis differed in spatiotemporal distribution, which was not previously noted. In addition, in our study, Fas/FasL-mediated killing played a major role in T cell-induced mucosal damage, whereas Merger *et al.* (17) indicated that the absence of Fas/FasL did not reduce apoptosis. This discrepancy may be due to differences in the dose of antibody used. In various studies, antibody was injected intravenously at relatively high doses (from 50 to 400 μg per mouse), whereas we used a dose of 12.5 μg per mouse intraperitoneally (17, 33, 34). At this dose, the number of apoptotic cells had already reached the maximum value (Fig. 1B and C). However, we also observed that the intestinal tissue damage that developed in our experimental setting was milder and recovered more rapidly than that at higher antibody doses (data not shown). Further, in contrast to previous studies, serum TNF-α was not detected at any time point up to 24 h after the injection (data not shown; detection limit: 50 pg ml^{-1}). These data suggest that the Fas/FasL pathway is important for the T cell-mediated IEC apoptosis following a weaker stimulation by anti-CD3 and that higher doses of the antibody stimulate various additional immunological responses and result in more complicated, long-term and serious enteropathy. Nonetheless, other cytotoxic pathways, for example perforin, suggested to be a very important cytotoxic pathway by Merger *et al.* (17), may contribute to IEC apoptosis in the present study because it was incompletely inhibited in the absence of Fas (in *lpr/lpr* mice). Thus, our protocol may be useful to discriminate and analyze the involvement of different cytotoxic mechanisms causing intestinal damage.

In the present study, in addition to the analysis using *lpr/lpr* mice, we quantified the Fas-mediated killing activity of lymphocytes from different compartments isolated from mice administered anti-CD3 antibody and found that the enhanced cytotoxicity of IEL and SPL was seen at different times. The enhanced killer activity of IEL and SPL at different times may, therefore, result in the induction of apoptosis at different times and sites. Complete abrogation of both phases of apoptosis in nude mice suggests an essential contribution of thymus-derived T cells. Indeed, αβIEL, which contain a large portion of thymus-derived T cells, showed stronger killer activity than γδIEL, which consist mainly of gut-derived T cells (data not shown). These data suggest the hypothesis that the first phase of apoptosis is mediated mainly by thymus-derived IEL and the second phase is mediated by peripheral lymphocytes. Lymphocyte transfer experiments provided data that were, at least partially, consistent with this hypothesis. Namely, the adoptive transfer of SPL from euthymic mice to nude mice before anti-CD3 injection resulted in only the second phase of apoptosis, whereas IEL caused both (Fig. 8). Compared with anti-CD3 antibody-induced apoptosis in euthymic mice, the apoptosis induced in IEL-engrafted nude mice was more prominent in the villus at 24 h (Figs 7 and 8, experiment 2). This discrepancy remains to be clarified in the future, but the following should be considered. The rapid massive villous apoptosis induced in euthymic mice resulted in an extensive loss of intestinal villus by 24 h and, therefore, the number of observable villous apoptotic bodies may have decreased. A relatively longer villus (i.e. greater integrity) was observed in the intestine of dual-grafted nude mice (data not shown).

The concomitant transfer of IEL and SPL abrogated the SPL-induced second phase of apoptosis, but SPL transfer at 5 weeks after IEL transfer had an additive effect on the second phase of apoptosis at 24 h (Fig. 8). Clarification of this discrepancy also requires further investigation but may be explained by the following. In experiment 1, a substantial amount of transferred IEL may have accumulated in the spleen because the cells did not have sufficient time to repopulate

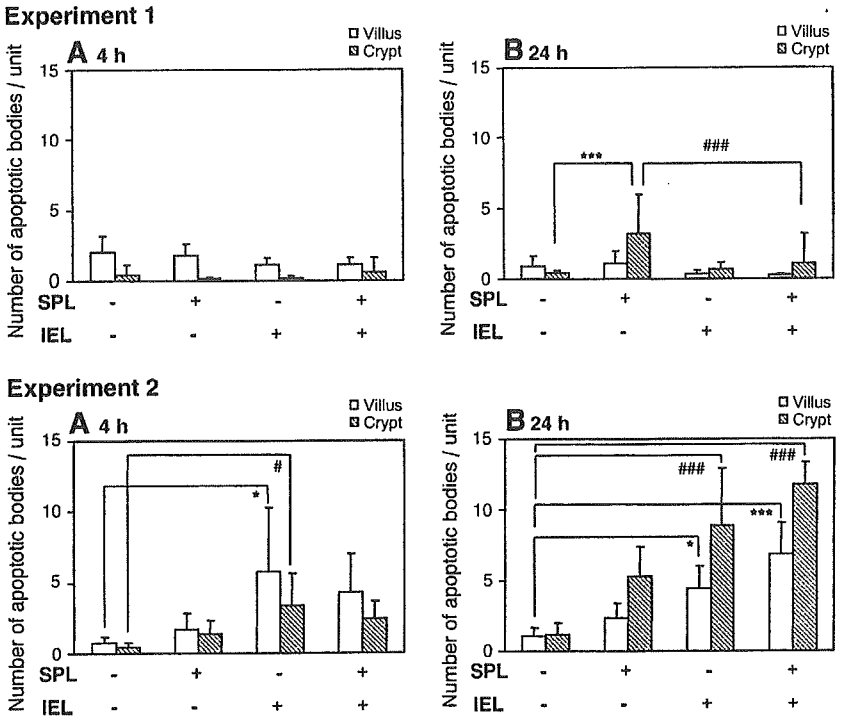

Fig. 8. Adoptive transfer of BALB/c IEL and SPL into BALB/c *nu/nu* mice. Experiment 1: naive nude mice were respectively or serially injected with SPL (5×10^7) and IEL (1×10^7). The day after the transfer, anti-CD3 was administered at a dose of 12.5 μg per mouse. The number of apoptotic cells 4 (A) and 24 h (B) after antibody administration is shown (number of mice = 5–13). The experiment was repeated twice with similar results. When SPL and/or IEL were transferred into the mice without anti-CD3 administration, the number of apoptotic bodies was <1.5 for all graft groups. Data represent means ± SD per villus per crypt unit. ***$P < 0.0005$ versus non-transferred in crypt; ###$P < 0.0005$ versus SPL transferred alone in crypt. Experiment 2: IEL (1×10^7) from 6- to 11-week-old-BALB/c mice were transferred to BALB/c *nu/nu* mice of the same age. After 5 weeks, saline or SPL (5×10^7) was transferred to the IEL-grafted or naive BALB/c *nu/nu* mice, and on the next day anti-CD3 was administered at a dose of 12.5 μg per mouse. The number of apoptotic cells 4 (A) and 24 h (B) after antibody administration is shown (number of mice = 5–6). When SPL and/or IEL without anti-CD3 administration were transferred to the mice, the number of apoptotic bodies was <1.5 for all graft groups. Data represent means ± SD per villus per crypt unit. *$P < 0.05$ and ***$P < 0.0005$ versus non-transferred in the villus; #$P < 0.05$ and ###$P < 0.0005$ versus non-transferred in the crypt.

the intestinal epithelium. In such a case, upon CD3 activation, $FasL^+$IEL may kill Fas^+SPL, including dendritic cells, which would result in the suppression of any T cell activation. By contrast, in experiment 2, many of the transferred IEL will have migrated into the intestine by 5 weeks after transfer, and therefore, the killing of SPL by IEL in the spleen may not occur when anti-CD3 antibody is injected. The killer activity of both IEL and SPL can thus be expressed additively, resulting in the observed enhanced killing of IEC.

It has been reported that 78.9% of IEC express the Fas molecule and the expression is not uniform (11). In addition, the sensitivity of cell death may be different between the villus and crypt because P53-independent cell death occurred by ischemia-reperfusion is induced in the villus to a greater extent than in the crypt (20). One explanation for bi-phasic apoptosis may be that villous IEC is more sensitive than crypt IEC for FasL signaling. The differences in the sensitivity of IEC to apoptosis may contribute to the bi-phasic apoptosis when mediated by IEL, especially. However, this hypothesis appears unsatisfactory because it does not provide a full explanation of the data presented in Figure 8, experiments 1 and 2, in that the anti-CD3-injection to SPL-grafting nude mice resulted in the second phase apoptosis only.

In summary, we have described a model of small intestinal injury induced by systemic T cell activation and characterized by IEC apoptosis with at least two distinct phases mediated mainly by the Fas/FasL system of thymus-derived T cells. Differential involvement of both peripheral and mucosal lymphocytes in the induction of the apoptosis has been demonstrated. Despite the many unresolved issues raised by these experiments, the demonstration of the possible involvement of different T cell compartments and their interactions in IEC apoptosis provides an important advance and useful tools in the effort to determine the components and mechanisms by which immune responses are regulated in normal and pathological intestinal mucosa.

Acknowledgements

The authors thank Dr Yasuhiro Komatsu, an ex-chief manager of Kampo & Pharmacognosy Laboratory of Tsumura & Co., for his valuable discussions.

Abbreviations

DEAE	diethylaminoethyl
E/T	Effecter/Target
FasL	Fas ligand
H&E	hematoxylin and eosin
IEC	intestinal epithelial cells
IEL	intestinal intraepithelial lymphocytes
MLNC	mesenteric lymph node cells
PPL	Peyer's patch lymphocytes
SPL	splenocytes
TNF	tumor necrosis factor
TUNEL	terminal deoxynucleotidyl transferase-mediated dUTP nick-end labeling

References

1 Fiocchi, C. 1998. Inflammatory bowel disease: etiology and pathogenesis. *Gastroenterology* 115:182.
2 Radford-Smith, G. 1997. Ulcerative colitis: an immunological disease? *Bailliere's Clin. Gastroenterol.* 11:35.
3 Schuppan, D. 2000. Current concepts of celiac disease pathogenesis. *Gastroenterology* 119:234.
4 Ueyama, H., Kiyohara, T., Sawada, N. *et al.* 1998. High Fas ligand expression on lymphocytes in lesions of ulcerative colitis. *Gut* 43:48.
5 Suzuki, A., Sugimura, K., Ohtsuka, K. *et al.* 2000. Fas/Fas ligand expression and characteristics of primed CD45RO+ T cells in the inflamed mucosa of ulcerative colitis. *Scand. J. Gastroenterol.* 35:1278.
6 Ciccocioppo, R., Di Sabatino, A., Parroni, R. *et al.* 2000. Cytolytic mechanisms of intraepithelial lymphocytes in coeliac disease (CoD). *Clin. Exp. Immunol.* 120:235.
7 Di Sabatino, A., D'Alo, S., Millimaggi, D. *et al.* 2001. Apoptosis and peripheral blood lymphocyte depletion in coeliac disease. *Immunology* 103:435.
8 Di Sabatino, A., Ciccocioppo, R., D'Alo, S. *et al.* 2001. Intraepithelial and lamina propria lymphocytes show distinct patterns of apoptosis whereas both populations are active in Fas based cytotoxicity in coeliac disease. *Gut* 49:380.
9 Ciccocioppo, R., Di Sabatino, A., Parroni, R. *et al.* 2001. Increased enterocyte apoptosis and Fas-Fas ligand system in celiac disease. *Am. J. Clin. Pathol.* 115:494.
10 Ciccocioppo, R., D'Alo, S., Di Sabatino, A. *et al.* 2002. Mechanisms of villous atrophy in autoimmune enteropathy and coeliac disease. *Clin. Exp. Immunol.* 128:88.
11 Sakai, T., Kimura, Y., Inagaki-Ohara, K., Kusugami, K., Lynch, D. H. and Yoshikai, Y. 1997. Fas-mediated cytotoxicity by intestinal intraepithelial lymphocytes during acute graft-versus-host disease in mice. *Gastroenterology* 113:168.
12 Bonhagen, K., Thoma, S., Leithauser, F., Moller, P. and Reimann, J. 1998. A pancolitis resembling human ulcerative colitis (UC) is induced by CD4+ TCR alphabeta T cells of athymic origin in histocompatible severe combined immunodeficient (SCID) mice. *Clin. Exp. Immunol.* 112:443.
13 Miwa, K., Hashimoto, H., Yatomi, T., Nakamura, N., Nagata, S. and Suda, T. 1999. Therapeutic effect of an anti-Fas ligand mAb on lethal graft-versus-host disease. *Int. Immunol.* 11:925.
14 Kataoka, Y., Iwasaki, T., Kuroiwa, T. *et al.* 2001. The role of donor T cells for target organ injuries in acute and chronic graft-versus-host disease. *Immunology* 103:310.
15 Arnold, D., Wasem, C., Juillard, P. *et al.* 2002. IL-18-independent cytotoxic T lymphocyte activation and IFN-gamma production during experimental acute graft-versus-host disease. *Int. Immunol.* 14:503.
16 Mowat, A. M. and Vinley, J. L. 1997. The anatomical basis of intestinal immunity. *Immunol. Rev.* 156:145.
17 Merger, M., Viney, J. L., Borojevic, R. *et al.* 2002. Defining the roles of perforin, Fas/FasL, and tumour necrosis factor alpha in T cell induced mucosal damage in the mouse intestine. *Gut* 51:155.
18 Tsuzuki, T., Yoshikai, Y., Ito, M., Mori, N., Ohbayashi, M. and Asai, J. 1994. Kinetics of intestinal intraepithelial lymphocytes during acute graft-versus-host disease in mice. *Eur. J. Immunol.* 24:709.
19 Okudela, K., Ito, T., Mitsui, H. *et al.* 1999. The role of p53 in bleomycin-induced DNA damage in the lung. A comparative study with the small intestine. *Am. J. Pathol.* 155:1341.
20 Coopersmith, C. M., O'Donnell, D. and Gordon, J. I. 1999. Bcl-2 inhibits ischemia-reperfusion-induced apoptosis in the intestinal epithelium of transgenic mice. *Am. J. Physiol.* 276:G677.
21 Pritchard, D. M. and Watson, A. J. 1996. Apoptosis and gastrointestinal pharmacology. *Pharmacol. Ther.* 72:149.
22 Taguchi, T., McGhee, J. R., Coffman, R. L. *et al.* 1990. Analysis of Th1 and Th2 cells in murine gut-associated tissues. Frequencies of CD4+ and CD8+ T cells that secrete IFN-gamma and IL-5. *J. Immunol.* 145:68.
23 Lin, T. S., Brunner, T., Tietz, B. *et al.* 1998. Fas ligand-mediated killing by intestinal intraepithelial lymphocytes—participation in intestinal graft-versus-host disease. *J. Clin. Investig.* 101:570.
24 Ramsdell, F., Seaman, M. S., Miller, R. E., Tough, T. W., Alderson, M. R. and Lynch, D. H. 1994. gld/gld mice are unable to express a functional ligand for Fas. *Eur. J. Immunol.* 24:928.
25 Yamamoto, M., Ogawa, K., Morita, M., Fukuda, K. and Komatsu, Y. 1996. The herbal medicine Inchin-ko-to inhibits liver cell apoptosis induced by transforming growth factor beta 1. *Hepatology* 23:552.
26 Yukawa, M., Iizuka, M., Horie, Y. *et al.* 2002. Systemic and local evidence of increased Fas-mediated apoptosis in ulcerative colitis. *Int. J. Colorectal Dis.* 17:70.
27 Inagaki-Ohara, K., Nishimura, H., Sakai, T., Lynch, D. H. and Yoshikai, Y. 1997. Potential for involvement of Fas antigen Fas ligand interaction in apoptosis of epithelial cells by intraepithelial lymphocytes in murine small intestine. *Lab. Investig.* 77:421.
28 Ellenhorn, J. D., Hirsch, R., Schreiber, H. and Bluestone, J. A. 1988. *In vivo* administration of anti-CD3 prevents malignant progressor tumor growth. *Science* 242:569.
29 Hirsch, R., Eckhaus, M., Auchincloss, H., Jr., Sachs, D. H. and Bluestone, J. A. 1988. Effects of *in vivo* administration of anti-T3 monoclonal antibody on T cell function in mice. I. Immunosuppression of transplantation responses. *J. Immunol.* 140:3766.
30 Hirsch, R., Gress, R. E., Pluznik, D. H., Eckhaus, M. and Bluestone, J. A. 1989. Effects of *in vivo* administration of anti-CD3 monoclonal antibody on T cell function in mice. II. *In vivo* activation of T cells. *J. Immunol.* 142:737.
31 Poussier, P., Edouard, P., Lee, C., Binnie, M. and Julius, M. 1992. Thymus-independent development and negative selection of T cells expressing T cell receptor alpha/beta in the intestinal epithelium: evidence for distinct circulation patterns of gut- and thymus-derived T lymphocytes. *J. Exp. Med.* 176:187.
32 Suzuki, S., Sugahara, S., Shimizu, T. *et al.* 1998. Low level of mixing of partner cells seen in extrathymic T cells in the liver and intestine of parabiotic mice: its biological implication. *Eur. J. Immunol.* 28:3719.
33 Ferran, C., Dy, M., Sheehan, K. *et al.* 1991. Inter-mouse strain differences in the *in vivo* anti-CD3 induced cytokine release. *Clin. Exp. Immunol.* 86:537.
34 Ferran, C., Dy, M., Sheehan, K. *et al.* 1991. Cascade modulation by anti-tumor necrosis factor monoclonal antibody of interferon-gamma, interleukin-3 and interleukin-6 release after triggering of the CD3/T cell receptor activation pathway. *Eur. J. Immunol.* 21:2349.

Available online at www.sciencedirect.com

SCIENCE DIRECT®

Gynecologic Oncology 97 (2005) 243–245

Gynecologic Oncology

www.elsevier.com/locate/ygyno

Case Report

Primary omental gestational choriocarcinoma ascertained by deoxyribonucleic acid polymorphism analysis

Kaoru Sakumoto*, Yutaka Nagai, Morihiko Inamine, Koji Kanazawa

Department of Obstetrics and Gynecology, Faculty of Medicine, University of the Ryukyus, Okinawa, Japan

Received 28 May 2004
Available online 1 February 2005

Abstract

Background. Abdominal choriocarcinoma is extremely rare. It is important to examine whether the disease is primary or metastatic and gestational or non-gestational.

Case. A 26-year-old nulli-gravid woman underwent laparoscopy for presumed ectopic pregnancy. The uterus, ovaries and fallopian tubes surrounded by hemoperitoneum were unremarkable. A hemorrhagic 7-cm-sized tumor was identified on the greater omentum and excised. Histology was consistent with choriocarcinoma. Analysis of human leucocyte antigen (HLA) gene polymorphism on deoxyribonucleic acid (DNA) demonstrated that tumor DNA contained both HLA locus antigens of patient and of her husband. Clinical remission was achieved with six courses of chemotherapy.

Conclusion. To our knowledge, this is the first reported case of choriocarcinoma that occurred primarily on the omentum ascertained to be of gestational origin by DNA polymorphism analysis.

Keywords: Choriocarcinoma; DNA polymorphism analysis; Omentum

Introduction

Primary abdominal gestational choriocarcinoma is an extremely rare malignancy [1,2]. When a patient with abdominal choriocarcinoma is encountered, it is clinically important to examine whether the disease developed primarily there or metastasized secondarily there from genital choriocarcinoma and whether the disease is of gestational origin or of non-gestational germ cell origin.

Case

A 26-year-old nulli-gravid woman presented to our hospital with low abdominal pain and genital bleeding, 7 weeks after her last menstrual period. She had a history of regular menstruation and married 1 year earlier. A urinary pregnancy test was positive, indicating her first pregnancy. Physical examination revealed rebound tenderness in the lower abdomen. Inspection with a bivalve vaginal speculum demonstrated a closed cervical os with bloody discharge. Transvaginal ultrasonography showed free cul-de-sac fluid with no intrauterine gestational sac. Non-clotting blood was obtained by culdocentesis. The serum human chorionic gonadotropin (hCG) level was 103,704 mIU/mL.

Laparoscopy, performed for a presumed diagnosis of aborted or ruptured ectopic pregnancy, disclosed the uterus and bilateral adnexa surrounded by hemoperitoneum. After suction of intraperitoneal blood (approximately 650 mL), the uterus, tubes and ovaries were visualized completely and confirmed to be entirely normal in appearance. No bleeding lesions or injuries were found on the peritoneal surface of the genital structures and the pelvic cavity. Laparoscopic observation turned to the upper abdominal cavity. A hemorrhagic, dark reddish friable tumor, measuring 7.0 ×

* Corresponding author. Department of Obstetrics and Gynecology, Faculty of Medicine, University of the Ryukyus, 207 Uehara, Nishihara-Machi, Nakagami-Gun, Okinawa, Japan. Fax: +81 98 895 1426.
E-mail address: sakumoto@med.u-ryukyu.ac.jp (K. Sakumoto).

0090-8258/$ - see front matter © 2004 Elsevier Inc. All rights reserved.
doi:10.1016/j.ygyno.2004.09.036

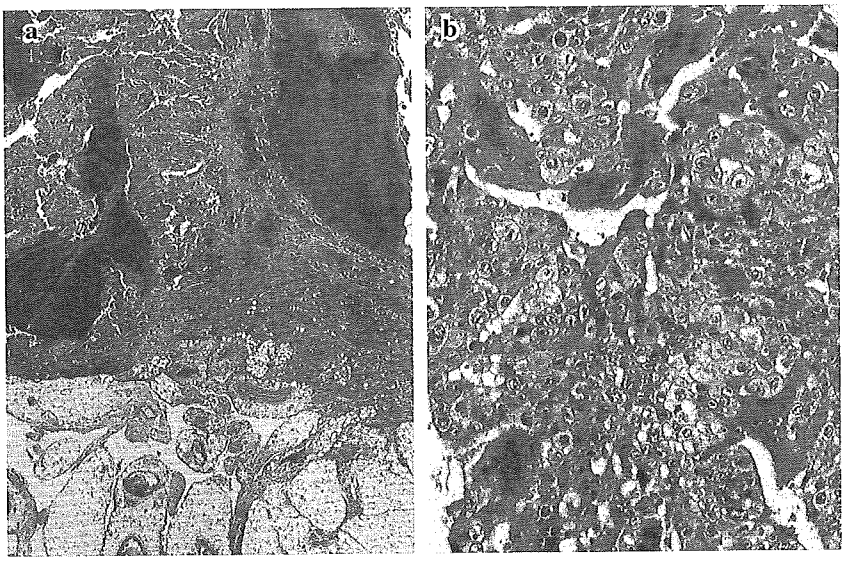

Fig. 1. Sheets and masses of tumor cells are seen in extensive hemorrhage and necrosis. On the bottom, the boundary with preserved omental fatty tissues circumscribes the tumor (a; hematoxylin–eosin, ×12). Cytotrophoblast, syncytiotrophoblast and intermediate trophoblast are present with no chorionic villi (b; hematoxylin–eosin, ×200).

5.0 × 4.5 cm, was seen on the right side surface of the greater omentum. The tumor was removed carefully along with the attached omental tissues under laparotomy. In addition, endometrial curettage was performed.

Histological examination of the resected tumor demonstrated a typical choriocarcinoma characterized by masses and sheets of markedly atypical trophoblastic cells with no component of chorionic villi, accompanied by extensive hemorrhage and necrosis (Fig. 1). No gestational tissues were noted in the endometrial specimen. Analysis of human leucocyte antigen (HLA) DRB gene polymorphism on deoxyribonucleic acids (DNAs) from tumor tissue, patient's leucocyte and her husband's leucocyte demonstrated that the tumor DNA contained both HLA DRB gene locus antigens of patient and of her husband (Fig. 2).

Her postoperative recovery was uneventful and serum hCG level declined to 350 mIU/mL 3 weeks later. No pulmonary or other distant metastases developed. Chemotherapy was given with a combination of methotrexate, actinomycin D and cyclophosphamide. Clinical remission was achieved with four courses of chemotherapy that were followed by two additional courses after normalization of hCG level. She has been healthy over 10 years with two healthy children.

Discussion

Recently, two interesting cases of abdominal extragenital or heterotopic gestational choriocarcinoma were reported. Bailey et al. [1] described a case of gestational choriocarcinoma occurring primarily on the left anterior abdominal wall of the pelvis, and Chen et al. [2] reported a case of gestational choriocarcinoma occurring primarily on the surface of subserosal uterine leiomyoma. They demonstrated that these

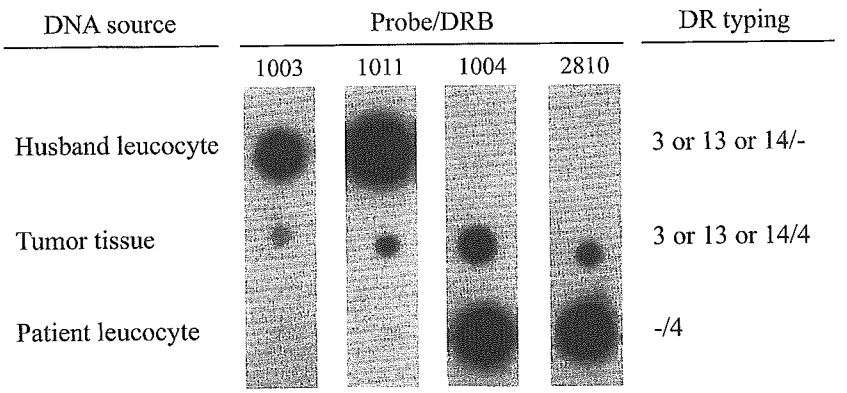

Fig. 2. Polymerase chain reaction-dot blot analysis with sequence-specific oligonucleotides targeted to the HLA DRB gene yielded the definite typing of tumor, patient and her husband.

cases were choriocarcinomas 'primarily' occurring at the disease sites, based on the appearance of the intact uterus or uterine cavity, tubes and ovaries free from pregnancy- or trophoblastic-tumor-associated findings. Our case also appears to be choriocarcinoma 'primarily' developing on the omental surface because of the same findings as those observed in their cases.

It is important to ascertain the mode of origin of choriocarcinoma because chemotherapy selection is contingent upon whether the tumor is of gestational versus non-gestational derivation. For example, it is described that gestational choriocarcinoma has a significantly better therapeutic response and prognosis than does non-gestational ovarian choriocarcinoma [3]. The authors of two previous case reports suggested that their cases were 'of gestational origin' arising from a conceptus in newly developed pregnancy, based on the patient's history of pregnancy signs after a missed normal menstrual period. Their suggestion seems to be reasonable, furthermore because nongestational choriocarcinoma is a rare malignant teratoid tumor that occurs mainly in the ovary of prepubescent children or adults younger than 20 years of age and that is usually admixed with other germ cell tumor elements, such as dysgerminoma, teratoma or yolk sac tumor [4,5]. In our case, an analysis of HLA gene polymorphism demonstrated that the tumor contained the allele from the patient's husband in addition to her allele, indicating the possibility that the tumor is of gestational origin, and not of parthenogenetic origin [6].

Although gestational choriocarcinoma is usually recognized following the sequel of such other trophoblastic products of conception as hydatidiform mole, abortion and pre-term or term pregnancy, it is described that primitive previllous trophoblasts may alternate directly with malignant trophoblasts [7]. Acosta-Sisson [8] termed such a case "choriocarcinoma ab initio" and cited clinical observations suggesting the existence of such a pathogenetic course. On the other hand, Friedrich [9] reported primary omental pregnancy, although it probably resulted from regurgitation and migration of an ovum that was fertilized in the tube. Thus, our case seems to be gestational choriocarcinoma that arose immediately from early-stage trophoblasts of a new conceptus that was implanted on the omentum. To our knowledge, this is the first reported case of choriocarcinoma that occurred primarily on the surface of the greater omentum and that was ascertained to be of gestational origin by HLA polymorphism analysis of tumor tissue.

Acknowledgment

The authors thank Professor Norio Wake (Department of Reproductive Physiology and Endocrinology, Kyushu University) for his kind assistance with outstanding study on DNA polymorphism analysis.

References

[1] Bailey JL, Hinton EA, Ashfaq R, Schorge JO. Primary abdominal gestational choriocarcinoma. Obstet Gynecol 2003;102:988–90.
[2] Chen M-J, Yang J-H, Lin M-C, Ho H-N, Yang Y-S. An unusual gestational choriocarcinoma occurring primarily on the surface of a subserous leiomyoma. Br J Obstet Gynaecol 2004;111:188–90.
[3] Dehner LP. Gestational and nongestational trophoblastic neoplasia: a historic and pathobiologic survey. Am J Surg Pathol 1980;4:43–58.
[4] Nogales FF. Germ cell tumours of the ovary. In: Fox H, Wells M, editors. Haines and Taylor obstetrical and gynecological pathology, fourth ed. New York: Churchill Livingstone, 1995. p. 861–2.
[5] Talerman A. Germ cell tumors of the ovary. In: Kurman RJ, editor. Blaustein's pathology of the female genital tract, fifth ed. New York: Splinger-Verlag, 2002. p. 992–4.
[6] Arima T, Imamura T, Sakuragi N, Higashi M, Kamura T, Fujimoto S, Nakano H, Wake N. Malignant trophoblastic neoplasms with different modes of origin. Cancer Genet Cytogenet 1995;85:5–15.
[7] Hertz R. Spectrum of gestational trophoblastic disease. In: Hertz R, editor. Choriocarcinoma and related gestational trophoblastic tumors in women. New York: Raven Press, 1978. p. 13–22.
[8] Acosta-Sisson H. Can the implanting trophoblasts of the fertilized ovum develop immediately into chorionepithelioma? Am J Obstet Gynecol 1955;69:442–6.
[9] Friedrich MA. Primary omental pregnancy: 2 cases of primary peritoneal pregnancy. Obstet Gynecol 1968;31:104–9.

J. Perinat. Med. 33 (2005) 199–205 • Copyright © by Walter de Gruyter • Berlin • New York. DOI 10.1515/JPM.2005.037

Original articles – Obstetrics

Cerebral edema on MRI in severe preeclamptic women developing eclampsia

Hideo Matsuda*, Kenichiro Sakaguchi, Tomoko Shibasaki, Hironori Takahashi, Yuichi Kawakami, Kenichi Furuya and Yoshihiro Kikuchi

Department of Obstetrics and Gynecology, National Defense Medical College, Japan

Abstract

Objective: The aim of this study is to identify suitable applications for cerebral MR (magnetic resonance) scanning in cases of severe preeclampsia and eclampsia through comparison of clinical course and easily accessible parameters.

Methods: From January 2001 to December 2003, cerebral MR scans were performed on 43 women with severe preeclampsia; of those 41 were enrolled in data analyses. Twenty clinical parameters, including age, body mass index, blood pressure, liver and renal function, and coagulation status, were compared for each patient. Data were analyzed using the SPSS program on a VAX main frame.

Results: Among 41 severe preeclamptic women, abnormal MR images were observed in 11 cases including six with systemic seizures. Predictive accuracy of eclampsia with abnormal cerebral MR imaging was 84.9% ($P=0.00001$), while only 14.3% of severe preeclampsia cases had been diagnosed radiologically. Statistical analysis suggests diastolic BP and serum AST as predictive parameters for abnormal MR images with 82.9% predictive accuracy ($P=0.0007$).

Conclusions: Cerebral edema can be observed in preeclamptic patients developing eclampsia. Rapid delivery is indicated when diastolic BP and AST are elevated. MR scanning is useful when delivery is delayed due to fetal immaturityin cases of severe preeclampsia.

Keywords: Cerebral edema; eclampsia; MRI; posterior leukoencephalopathy; preeclampsia; pregnancy induced hypertension.

*Corresponding author:
Hideo Matsuda, MD
Department of Obstetrics and Gynecology
National Defense Medical College
3–2 Namiki, Tokorozawa
Saitama Prefecture
359-1513 Japan
Tel.: +81-42-995-1687
Fax: +81-42-996-5213
E-mail: hmatsuda@ndmc.ac.jp

Introduction

Eclampsia is defined as the new onset of convulsions during pregnancy or postpartum, unrelated to other cerebral pathologic conditions, in women with preeclampsia. Matter and Sibai [11] concluded that eclampsia remains a significant complication of pregnancy with high maternal mortality and morbidity rates, and that antepartum onset carries greater risks, with onset under 32 weeks' gestation being particularly dangerous to both mother and fetus. Thus, to predict the onset of eclampsia and start appropriate treatment as early as possible is important for favorable perinatal prognosis.

Brain magnetic resonance (MR) scans and MR angiographies are now widely used in various fields of clinical medicine, especially for hypertension, renal failure, and immunosuppressive medicine users. Reversible posterior leukoenchephalopathy is a typical finding in these patients, and it is also frequently observed in eclampsia patients. Weingarten [18] reported abnormal MR images in women with hypertensive encephalopathy including focal white matter lesions on the reversible generalized cerebral edema. Peterkin [14] reported that reversible cerebral MR abnormal images may be observed in severe preeclamptic women. However, these reports did not discuss when MR images should be taken, what clinical parameter is most reflective of maternal brain abnormality, or whether abnormal images always exist prior to the onset of eclampsia. Rutherford and colleagues [15] have studied the use of cerebral MRI in preeclampsia and concluded that it was not clinically useful when used routinely. MR scanning is an expensive imaging modality that requires patients to leave the area of care for a significant length of time and should therefore not be undertaken lightly.

This study was conducted in order to identify accessible clinical parameters for abnormal brain MR imaging in severe preeclampsia cases, and to identify appropriate applications for MR scanning in managing severe preeclampsia and eclampsia.

Methods

From January 1, 2001 to December 31, 2003, 92 patients with severe preeclampsia, as diagnosed under the guidelines of the National High Blood Pressure Education Program [13], were hospitalized and treated. Of those, 43 agreed to participate in

this study, and 2 subsequently dropped out because of their inability to undergo MR scanning due to claustrophobia. The remaining 41 were enrolled in data analyses. Magnesium sulfate prophylaxis (as per the Magpie trial [10] was used with all of these patients, and some were carefully treated with alpha methyldopa, labetalol hydrochloride, and calcium channel blockers such as nicardipine hydrochloride to await fetal maturation.

Maternal MR scans were performed on all patients without regard to headaches and visual symptoms in those with severe preeclampsia, and clinical data were recorded prior to MR scanning. Follow-up MR scans were repeated until the abnormal findings disappeared. Twenty clinical parameters, including age, body mass index, blood pressure, liver function, renal function, and coagulation status, were recorded for each patients. Magnetom Vision (Siemens, Germany) MR systems providing fluid-attenuated inversion recovery (FLAIR) sequences and diffusion-weighted images (DWI), were used. In DWI, calculation of apparent diffusion coefficient (ADC) map assessed the relationship between the diffusion constant from b-value of 0 s/mm^2 to b-value of 1000 s/mm^2, and b-value of 1000 s/mm^2 was specified as a measure of the diffusion sensitivity. Simultaneously, three-dimensional (3D) time-of-flight MR angiography (TOF MRA) was also applied. Each MR image was diagnosed by at least two radiologists.

Data were analyzed using the SPSS program on a VAX main frame.

Correlation of eclampsia and abnormal brain MR images was calculated with a χ^* test. An analysis of variance was performed in order to measure the variations between each of the parameters. Bonferroni tests comparisons were performed between the abnormal MR group and normal MR group, and between the eclampsia group and non-eclampsia group. The stepwise discriminant procedure was used in order to determine the relative contribution of each variable. Two clinical parameters, diastolic blood pressure (BP) and serum AST were subjected to both stepwise and direct discriminant analysis in order to calculate a specific discriminant formula. Expected abnormality detection with MRI was compared to the results of MR scanning with the χ^* test.

Results

All 41 women were treated with magnesium sulfate prophylaxis on their admission to the National Defense Medical College Hospital. Among the 41 severe preeclampsia patients, six had systemic seizures (all of the patients with seizure had been transferred from local regional clinics), and 14 cases had visual symptoms without retinal detachmnet. Patients with systolic blood pressure over 180 mmHg and diastolic blood pressure over 120 mmHg were treated with one or two kinds of antihypertensive drugs, such as alpha methyldopa, labetalol hydrochloride, and calcium channel blockers, with careful fetal monitoring prior to MR scanning. Urinary protein of more than 3.5 g/day was observed in 12 cases. Abnormal MR images were obtained for 11 cases (nine of vasogenic edema and two of minor cerebral embolisms), the suspected vasoconstriction was observed in four cases. As shown in Table 1, of the 11 cases with abnormal MR findings, two cases developed eclampsia within 2 h of delivery, four cases developed eclampsia between 12 and 48 h postpartum, and five cases had no seizures. Typical abnormal MR images are shown in Figure 1, Figure 2, and Figure 3.

A 2×2 table of our MRI findings and eclampsia was performed and a specificity of 100.0%, sensitivity of 85.7%, positive predictive value of 54.5%, negative predictive value of 100.0%, and prediction accuracy of 87.8% ($P=0.00001$) were obtained (Table 2). For eclampsia, brain MR images showed some abnormality (especially posterior leukoencephalopathy) as has been reported elsewhere, while abnormal MR images were obtained for only 14.3% (5/35) of women with severe preeclampsia who had no seizures. This suggests that cerebral damage could exist prior to the onset of seizure in severe preeclampsia. Four women were thought to show vasoconstriction in 3D-TOF-MRA, but two of the four were possible anatomical variations.

Bonferroni analysis was performed to detect important, easily accessible clinical parameters for eclampsia (Table 3) and abnormal MR images (Table 4). Diastolic blood pressure (measured before MR scanning) and serum AST, ALT, LDH, and serum creatinine were observed to have statistical significance, while other parameters, such as systolic blood pressure, urine protein, uric acid, and antithrombin III, were not. We ascertained that diastolic blood pressure has more clinical significance than systolic blood pressure, and more significance in elevated liver enzymes than in renal malfunction and coagulopathy, in preventing eclampsia among severe preeclamptic patients, whereas all parameter were more severe than those for normal pregnant women. Although statistically significant differences were observed, differences between normal and abnormal measurements within each parameter were relatively small, thus making it possible to determine what parameter combinations would best predict MRI abnormalities. We therefore conducted stepwise discriminant analysis in order to identify the most predictive parameter combination.

A 2×2 table of expected MR abnormalities and actual abnormal MR diagnosis was calculated using stepwise discriminant analysis. After deriving an appropriate canonical coefficient, diastolic blood pressure and serum AST levels were selected. As shown in Table 5, this combination of parameters produced the best result statistically, with a prediction accuracy of 82.9% ($P=0.0007$). These two parameters were found to correlate with abnormal MR findings, although it is difficult to analyze the cut-off levels with these parameters with small data samples.

The time course of abnormal cerebral MR images is shown in Table 6. Prolonged elevated diastolic pressure and general fatigue were observed in case 1 and case 8, who suffered coma after seizures, and several MR scans were required to confirm "reversible" leukoencephalopathy. Rapid recoveries were observed after delivery in the remaining cases. 3D-TOF-MRA detected some sus-

Table 1 Characteristics of participants and MRI findings.

Case	Age	BP (mmHg)	UP (g/day)	Headaches	Visual symptoms	Seizures	MR diagnosis	Vasoconstriction
1	36	180/100	0.3	(+)	(+)	(+)	multi-lobal vasogenic edema, minimal infarction	suspected left ACA
2	31	170/120	18.2	(+)	(−)	(−)	posterior leukoencephalopathy	n.f.
3	35	180/122	0.3	(−)	(+)	(+)	basal ganglia vasogenic edema	n.f.
4	28	182/108	0.3	(+)	(+)	(+)	multi-lobal edema	right CA
5	29	163/120	0.1	(−)	(+)	(−)	n.f.	suspected right MCA
6	23	180/110	10.4	(−)	(+)	(+)	multi-lobal vasogenic edema, minimal infarction	n.f.
7	36	191/106	0.3	(+)	(+)	(+)	temporal and posterior leukoencephalopathy	n.f.
8	38	192/120	6.3	(+)	(+)	(−)	posterior encephalopathy	n.f.
9	28	180/110	1.7	(+)	(−)	(+)	multi-lobal edema	n.f.
10	38	170/100	10.0	(−)	(+)	(−)	n.f.	blt. ACA/PCA
11	32	170/110	7.6	(−)	(−)	(−)	basal ganglia vasogenic edema	n.f.
12	42	160/ 90	0.2	(−)	(+)	(−)	n.f.	n.f.
13	31	212/106	0.7	(−)	(+)	(−)	n.f.	n.f.
14	19	160/ 80	0.8	(−)	(+)	(−)	n.f.	n.f.
15	32	200/100	1.7	(−)	(+)	(−)	n.f.	n.f.
16	27	170/100	5.5	(−)	(+)	(−)	n.f.	n.f.
17	40	182/104	3.0	(−)	(−)	(−)	n.f.	n.f.
18	27	160/ 90	2.9	(−)	(−)	(−)	n.f.	n.f.
19	33	168/ 80	1.7	(−)	(−)	(−)	n.f.	n.f.
20	37	172/110	4.8	(−)	(−)	(−)	n.f.	n.f.
21	29	160/103	0.3	(−)	(−)	(−)	n.f.	n.f.
22	24	176/ 98	10.1	(−)	(−)	(−)	n.f.	n.f.
23	31	160/104	3.8	(−)	(−)	(−)	n.f.	n.f.
24	32	160/100	2.5	(−)	(−)	(−)	n.f.	n.f.
25	34	212/110	0.7	(−)	(+)	(−)	n.f.	n.f.
26	35	180/ 90	0.8	(−)	(−)	(−)	n.f.	n.f.
27	37	194/134	0.4	(−)	(−)	(−)	n.f.	n.f.
28	34	150/100	0.9	(−)	(−)	(−)	n.f.	n.f.
29	31	169/100	6.8	(−)	(−)	(−)	n.f.	n.f.
30	26	185/105	0.4	(−)	(−)	(−)	n.f.	n.f.
31	34	170/100	2.7	(−)	(−)	(−)	n.f.	n.f.
32	32	160/ 90	4.0	(−)	(−)	(−)	n.f.	n.f.
33	30	182/120	1.6	(−)	(−)	(−)	n.f.	n.f.
34	27	174/118	3.8	(−)	(−)	(−)	n.f.	n.f.
35	32	172/110	0.8	(−)	(−)	(−)	n.f.	n.f.
36	35	186/106	1.4	(−)	(−)	(−)	n.f.	n.f.
37	34	160/108	0.7	(−)	(−)	(−)	n.f.	n.f.
38	29	160/103	1.0	(−)	(−)	(−)	n.f.	n.f.
39	22	170/100	0.9	(−)	(−)	(−)	n.f.	n.f.
40	34	162/100	0.1	(−)	(−)	(−)	n.f.	n.f.
41	27	170/110	11.8	(−)	(−)	(−)	n.f.	n.f.

BP: Blood pressure prior to MR scans, UP: Urinary protein, n.f.: normal findings. ACA: anterior cerebral artery, CA: carotid artery, MCA: mid cerebral artery.

pected vasoconstrictions but the clinical significance of this was controversial for two reasons: First, temporary vasoconstrictions due to eclampsia could have been stabilized by magnesium sulfate and been difficult to visualize with MR angiography; and second, anatomical variations were frequently observed in the cerebral vasculature. As Rutherford [15] reported, MR angiography may be much less appropriate to assess the functional vascular condition and to monitor cerebral vasospasms than transcranial Doppler ultrasound. According to our data, abnormal MR angiography alone has poor reliability for ascertaining clinical significance.

Emergency cesarian sections were performed on 33 cases, labors were induced in five cases ending in vaginal delivery, and three cases delivered spontaneously. Neonatal prognoses were good for all women after some were transferred to the NICU. All women involved in the study finally recovered without sequelae.

Discussion

Abnormal cerebral images were detected in only 14.3% of severe preeclampsia cases, and so there is little

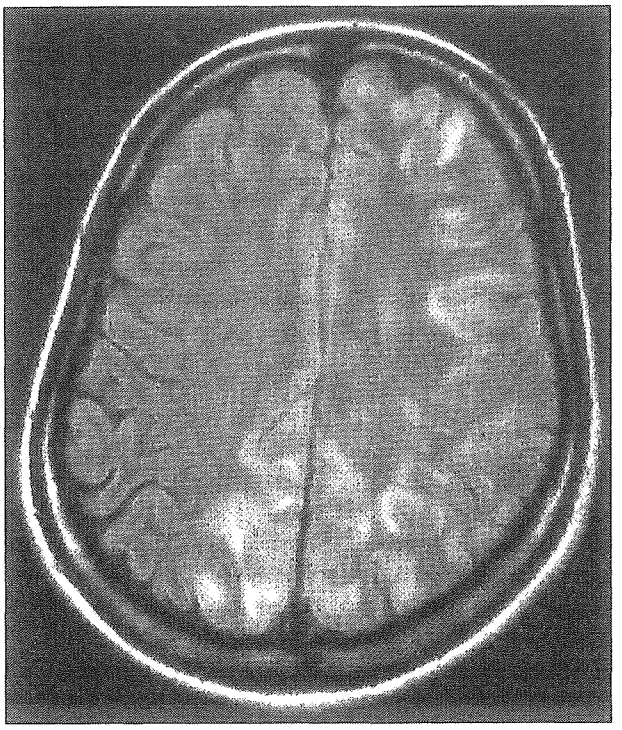

Figure 1 Fluid-attenuated inversion recovery (FLAIR) image showing parietal and occipital, but also some typical frontal lobe edema. (Case 1)

necessity to perform routine MR scanning on all severe preeclampsia patients. However, patients who show elevated diastolic blood pressure and liver enzymes should be recognized as possible candidates for eclampsia, even though appropriate treatments may already have been implemented. Emergency cesarian section prevented five women from developing eclampsia, according to their abnormal MR images. In the remaining six women, delivery may have been delayed too long because magnesium sulfate and emergency cesarian sections could not prevent these women from developing eclampsia.

From our data, we conclude that cerebral damage can occur without obvious symptoms in a number of severe preeclamptic women prior to developing eclampsia. Elevated diastolic blood pressure and liver enzymes, especially serum AST, may be predictive parameters. Frequent routine evaluations of clinical parameters are very important and earlier deliveries are highly recommended in severe preeclampsia cases before brain damage begins.

When prolonged hypertension and elevated liver enzymes are observed postpartum in such patients, MR scanning is recommended because medication differs according to the diffusion weighted images. In vasogenic edema, lowering blood pressure is necessary, while in cytotoxic edema, stabilizing blood pressure is recommended even if blood pressure is rather high. MR scanning during pregnancy due to severe preeclampsia might be useful in a limited number of situations when, in the second trimester, the pregnancy is being continued in a maternal intensive care unit until fetal maturation. Even with such a delayed delivery policy, emergency cesarian section may be inevitable when abnormal MR images are obtained.

Brain MR scanning is now used widely in various fields of clinical medicine. Peterkin et al. [14] documented eclampsia exhibiting peculiar MR images in 1992, and Brown et al. [4] reported abnormal brain radiological findings within computed tomography in 1988. In 1997, Morris et al. [12] and colleagues confirmed remarkable changes in the area of the posterior cerebral arteries in eclampsia after Hinchey et al. [8] identified reversible posterior leukoenchephalopathy syndrome for a partic-

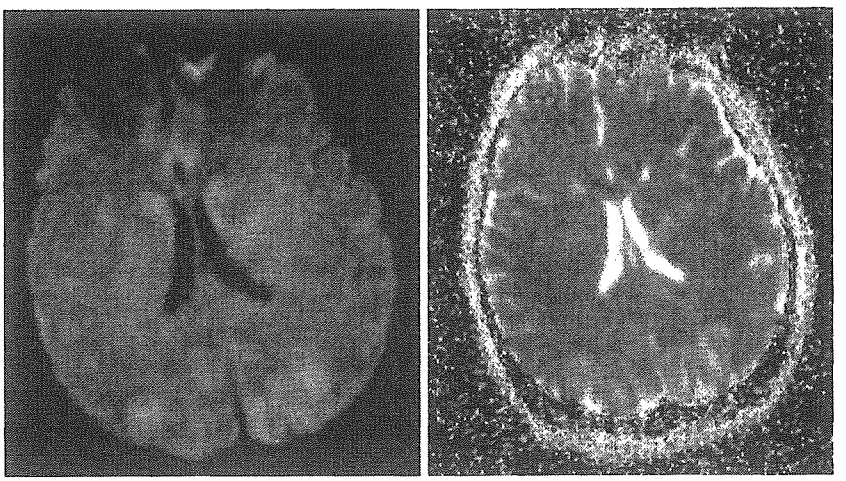

Figure 2 Vasogenic edema in posterior lobe. Right: Diffusion-weithted (DW) image (b-value: 1000 s/mm^2). Left: Apparent diffusion coefficient (ADC) map. (Case 8)

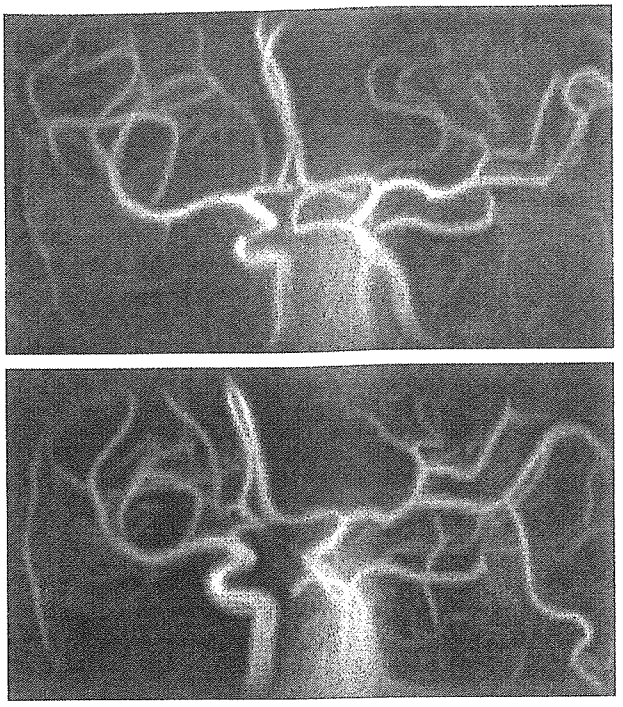

Figure 3 Above: Three-dimensional time-of-flight MR angiography (3D-TOF-MRA) showing vasoconstriction in right carotid artery. Below: Vasoconstriction was disappeared in 11 days. (Case 4)

ular type of brain edema in 1996. Thus, the cause of eclampsia is today believed to be cerebral edema. Cunningham and Twickler [6] thought that cerebral change is related to both ischemic (cytotoxic) and hyperperfusion (vasogenic) edema; conversely, Apollon et al. [2] used single-photon-emission computed tomography and provided evidence for hyperperfusion and vasogenic (hydrostatic) edema.

Using transcranial Doppler ultrasound, Williams and Wilson [19] determined that, in preeclampsia, increased cerebral perfusion pressure counterbalanced by increased cerebralovascular resistance is associated with no net change in cerebral blood flow. They concluded that loss of auto-regulation of cerebral blood flow manifesting as decreased vascular resistance eventually results in cerebral perfusion in eclampsia similar to that seen in hypertensive encephalopathy unrelated to pregnancy. Brackley et al. [3] showed that cerebral vasospasm in preeclamptic patients increased cerebral arterial wall stiffness and vasoconstriction. Rutherford et al. [15] reported that narrowing of cerebral vessels detectable on MR angiography does not occur commonly in preeclampsia, and MR spectroscopy results suggest that there is a relatively greater incidence of cerebral ischemia in preeclampsia cases than in normal pregnancy. Our data also suggested that 3D-TOF-MRA had less sensitivity and specificity than reported transcranial Doppler ultrasound. It is possible that cerebral change could already exist in preeclampsia cases and that preeclamptic women who have suffered a transient loss of cerebral vascular auto-regulation develop eclampsia.

Table 2 Prediction of eclampsia with MRI diagnoses.

	Eclampsia	Non-eclampsia
abnormal MRI	6	5
normal MRI	0	30

Sensitivity of 100.0%, specificity of 85.7%, positive predictive value of 54.5%, negative predictive value of 100.0%, and prediction accuracy of 87.8%. P=0.00001.

We hypothesized that abnormal cerebral MR images predict the onset of eclampsia in severe preeclamptic women. In our study 6 of 11 cases developed eclampsia, supporting this hypothesis, we believe the accumulation of cerebral damage can eventually result in lost hemodynamic auto-regulation and become visible in MR images in severe eclampsia cases as cerebral edema in particular, but not vasoconstriction. All six eclamptic women in our study had cerebral edema; however, from our small data sample it is impossible to suggest that severe preeclamptic women without abnormal MR images would not develop eclampsia. Although Cunningham et al. [6] reported a study in which only 10 of 175 eclamptic women demonstrated cerebral edema, it is thought that techanical progress may reveal visible cerebral damage in eclampsia.

Schwartz [17] showed that abnormal red blood cell morphology and serum LDH (lactic dehydrogenese) levels indicate cerebral edema in MR images, and blood pressure has no significant influence. Our results suggest that diastolic blood pressure and serum AST have considerable influence, while LDH does not. Today, diastolic blood pressure is accepted generally as a category of severity of preeclampsia, and serum AST is regarded as a diagnostic variable in HELLP syndrome. Jurgensen [9] reported a case of postpartum blindness caused by brain edema due to HELLP syndrome. In the present study, serum AST levels were derived as a variable in obtaining abnormal MR images, suggesting a relationship between parenchymal liver damage and brain edema. Cunningham et al. [5] described elevated serum AST levels in blindness associated with severe preeclampsia and eclampsia. Porostaglandins, nitric oxide, enodoterienes, vascular endotherial growth factors, genetic predisposition, immunological factors, inflammatory factors, etc, could have an important role in the severity of preeclampsia, but they are not easily accessed clinically. These patho-physiological tests are able to detect severe preeclampsia in pregnant women, but are no easily accessible marker to predict eclampsia when severe preeclampsia has not yet been established.

Antunes et al. [1] reported that radiological lesions compatible with transient white matter edema evolved

Table 3 Clinical parameters in eclampsia and non-eclampsia.

	Non-eclampsia (n=35)	Eclampsia (n=6)	P-value
serum ALT (IU/L)	19.2±3.24	95.4±41.1	0.0001*
serum LDH (IU/L)	289.0±19.0	738.0±327.7	0.0016*
serum AST (IU/L)	39.2±15.04	153.0±68.4	0.0143*
serum Creatinine (mg/dl)	0.6±0.02	0.81±0.13	0.0159*
Diastolic BP (mmHg)	104.2±2.44	114.4±3.39	0.0412*
Hematocrit (%)	34.3±1.42	36.3±2.78	0.0643
Systolic BP (mmHg)	175.2±2.76	182.7±3.40	0.14
Age (years old)	30.8±0.6	33.1±1.8	0.18
serum UA (mg/dl)	6.06±0.31	6.67±0.99	0.19
Body Mass Index (kg/m^2)	26.4±1.02	24.3±0.54	0.19
AT-3 (%)	90.9±3.20	80.0±5.87	0.23
D-dimer (mg/mL)	3.78±0.63	6.51±2.56	0.322
Platelet (×109/L)	200.4±1.3	183.7±3.7	0.37
urine Protein (g/day)	2.8±0.53	5.0±3.53	0.43
BUN (mg/dl)	10.9±1.03	13.3±2.90	0.48
GFR (mL/min)	109.1±6.2	97.2±15.2	0.51
serum Albumin (g/dl)	2.95±0.07	3.17±0.13	0.53
FDP (mg/mL)	8.1±1.06	10.1±2.76	0.58
serum Ca (mg/dl)	8.46±0.23	8.35±0.45	0.74
Fetal Body Weight (g)	2189.2±170.5	2228.3±189.1	0.81

* means statistical significant in Bonferroni test.

Table 4 Clinical parameters in abnormal MRI and normal MRI.

	Normal MRI (n=30)	Abnormal MRI (n=11)	P-value
Diastolic BP (mmHg)	102±2.0	114.0±2.0	0.0007*
sAST (IU/L)	25.0±3.0	138.1±56.1	0.0039*
sALT (IU/L)	21.0±4.1	56.3±26.1	0.0442*
sLDH (IU/L)	289±21.0	534±186.2	0.06
Hematocrit (%)	33.3±1.42	35.3±1.41	0.16
Systolic BP (mmHg)	174.2±2.72	180.2±3.41	0.16
Creatinine (mg/dl)	0.6±0.02	0.7±0.13	0.21
Age (years old)	30.8±1.41	32.1±1.33	0.88
U. Protein (g/day)	2.55±0.52	4.78±1.90	0.31
sCa (mg/dl)	8.4±0.22	8.4±0.31	0.35
D-dimer (mg/mL)	3.7±0.50	5.6±1.72	0.4
Platelet (×109/L)	200.4±1.31	223.7±2.42	0.46
UA (mg/dl)	6.2±0.21	7.4±0.99	0.73
sAlbumin (g/dl)	2.95±0.09	3.17±0.09	0.75
BUN (mg/dl)	11.9±1.03	12.3±2.40	0.78
AT-3 (%)	89.9±3.40	88.0±5.87	0.79
Fetal Body Weight (g)	2188.2±171.6	2230.3±199.2	0.80
GFR (mL/min)	118.1±7.2	105.2±10.2	0.84
Body Mass Index (kg/m^2)	26.4±1.02	26.3±1.04	0.86
FDP (mg/mL)	8.1±1.06	8.1±1.16	0.92

* means statistical signifficant in Bonferroni test.

Table 5 Prediction of abnormal MRI by stepwise discriminant analysis using diastolic BP and AST.

	Expected abnormal MRI	Expected normal MRI
true abnormal MRI	5	6
true normal MRI	1	29

Prediction accuracy of 82.9% was calculated. P=0.0007.

into leukomalacia, and Shwartz et al. [17] reported that posterior leukoencephalopathy is not always reversible. These reports concluded that immediate and appropriate treatment should be started. Garg et al. [7] emphasized that early recognition of posterior leukoencephalopathy is of paramount importance, as the prompt control of blood pressure can bring about a reversal of the syndrome. Delay in diagnosis and treatment can result in permanent damage to brain tissues. Schaefer et al. [16]

Table 6 Intervals of MRI scannings until the loss of abnormal images.

Case	MRI	Loss of abnormal findings	vasoconstriction	Loss of abnormal findings	Scanning (times)
1	multi-lobal vasogenic edema, minimal infarction	<12 days	left ACA (*suspected)	<380 days	6
2	posterior leukoencephalopathy	<15 days	(−)		2
3	basal ganglia vasogenic edema	<20 days	(−)		2
4	multi-lobal edema	<15 days	right CA	<12 days	2
5	(−)		right MCA (*suspected)	<132 days	2
6	multi-lobal vasogenic edema, minimal infarction	<92 days	(−)		3
7	temporal and posterior leukoencephalopathy	<30 days	(−)		2
8	posterior encephalopathy	<68 days	(−)		4
9	multi-lobal edema	<7 days	(−)		2
10	(−)		blt. ACA/PCA	<10 days	1
11	basal ganglia vasogenic edema	<30 days	(−)		2

ACA: anterior cerebral artery, CA: carotid artery, MCA: mid cerebral artery. *suspected: no denial of anatomical variation.

reported that diffusion-weighted imaging (DWI) could differentiate between vasogenic edema and cytotoxic edema, as well as between hypertensive encephalopathy and infarction, two different entities with different treatment protocols. They also emphasized that DWI should be performed on all eclamptic women as part of their evaluation.

It is thought that, as Rutherford et al. [15] concluded, MRI is not clinically cost-effective when used routinely in preeclampsia screening. However, MR scanning is to be recommended when a delayed delivery is chosen when fetal maturation in severe preeclampsia cases is desired, especially when the patient exhibits elevated diastolic blood pressure and elevated liver enzymes. In eclampsia cases, MR scanning is very useful and should be repeated until cerebral edema has disappeared.

References

[1] Antunes NL, TN Small, D George, F Boulad, E Lis: Posterior leukoencephalopathy syndrome may not be reversible. Pediatr Neurol 20(3) (1999 Mar) 241

[2] Apollon KM, JN Robinson, RB Schwartz, ER Norwitz: Cortical blindness in severe preeclampsia: Computed tomoguraphy, magnetic resonance imaging, and single-photon-emission computed tomography findings. Obstet Gynecol 95 (2000) 1017

[3] Brackley KJ, MM Ramsay, FB Pipkin, PC Rubin: The maternal cerebral circulation in preeclampsia: Investigations using Laplace transform analysis of Doppler waveforms. Br J Obstet Gynecol 107 (2000) 492

[4] Brown CEL, PD Purdy, FG Cunningham: Head computed tomographic scans in women with eclampsia. Am J Obstet Gynecol 159 (1988a) 915

[5] Cunningham FG, CO Fernandez, C Hernandez: Blindness associated with preeclampsia and eclampsia. Am J Obstet Gynecol 172 (1995) 1291

[6] Cunningham FG, D Twickler: Cerebral edema complicating eclampsia. Am J Obstet Gynecol 182 (2000) 94

[7] Garg RK: Posteriior leukoencephalopathy syndrome. Postgrad Med J 77 (2001) 24

[8] Hinchey J, C Chaves, B Appignani, J Breen, L Pao, A Wang, MS Pessin, C Lamy, JL Mas, LR Caplan: A reversible posterior leukoencephalopathy syndrome. N Engl J Med 334 (1996) 494

[9] Jurgensen JS, L Nibbe, KT Hoffmann, L Niehaus: Postpartum blindness. Lancet 358 (2001) 1338

[10] Magpie Trial Collaborative Group: Do Women with preeclampsia, and their babies, benefit from magnesium sulphate? The Magpie Trial: a randomized placebo-controlled trial. Lancet 359 (2002) 1877

[11] Matter F, BM Sibai: Eclampsia. Risk factors for maternal morbidity. Am J Obstet Gynecol 182 (2000) 307

[12] Morris MC, DM Twickler, MR Hatab, GD Clarke, RM Peshok, FG Cunnigham: Cerebral blood flow and cranial magnetic resonance imaging in eclampsia and severe preeclampsia. Obstet Gynecol 89 (1997) 561

[13] National High Blood Pressure Education Program: Working Group Report on High Blood Pressure in Pregnancy. Am J Obstet Gynecol 183 (2000) 51

[14] Peterkin IR, R Wee, RL Desmarais: Reversible cerebral, hepatic and renal lesions in severe preeclampsia. Can Assoc Radiol J 43(1) (1992 Feb) 60

[15] Rutherford JM, A Moody, S Crawshaw, PC Rubin: Magnetic resonance spectroscopy in preeclampsia: evidence of cerebral ischaemia. BJOG 110(4) (2003 Apr) 416

[16] Schaefer PW, FS Buonanno, RG Gonzalez, LH Schwamm: Diffusion-Weighted imaging discriminates between cytotoxic and vasogenic edema in a patient with eclampsia. Stroke 28 (1997) 1082

[17] Schwartz RB, SK Feske, JF Polak, U DeGirolami, A laia, KM Beckner, SM Bravo, RA Klufas, RYC Chai, JT Repke: Preeclampsia-Eclampsia: clinical and neuroradiographic correlates and insights into the pathogenesis of hypertensive encephalopathy. Radiology 217 (2000) 371

[18] Weingarten K, D Barbut, C Filippi, RD Zimmerman: Acute hypertensive encephalopathy: Findings on spin-echo and gradient-echo MR imaging. AJR 162 (1994) 664

[19] Williams KP, S Wilson: Persistence of cerebral hemodynamic changes in patients with eclampsia: a report of 3 cases. Am J Obstet Gynecol 181 (1999) 1162

Received October 14, 2004. Revised December 15, 2004. Accepted December 20, 2004.

BJOG: an International Journal of Obstetrics and Gynaecology
July 2004, Vol. 111, pp. 756–757

DOI: 10.1111/j.1471-0528.2004.00179.x

CASE REPORT

Intrauterine therapy for a cytomegalovirus-infected symptomatic fetus

Hideo Matsuda, Yuichi Kawakami, Kenichi Furuya, Yoshihiro Kikuchi

Case report

A 25 year old primigravida presented in July 2001 at 29 weeks of gestation with fetal hydrops. She had flulike symptoms three weeks earlier. On examination, she had no hypertension, proteinuria or any other abnormality. No blood group antibodies were detected. The fetal heart rates showed prolonged non-reassuring patterns on the non-stress test. Over 300 mL of ascites and hepatosplenomegaly were detected on ultrasonography. Maternal serum, amniotic fluid and fetal ascites revealed positive cytomegalovirus (CMV) DNA with quantitative real-time polymerase chain reaction (PCR). Repeated estimation of maternal serum CMV-specific IgM and IgG (enzyme immunoassay [EIA]) did not suggest primary CMV infection. No fetal brain abnormality (swelling, calcification and degeneration) was detected at her presentation with ultrasound and magnetic resonance scans. Percutaneous umbilical blood sampling showed fetal anaemia (haemoglobin: 10.5 g/dL), hypoproteinaemia (total protein: 3.8 g/dL) and elevated liver enzymes (γ-glutamyltranspeptidase: 1458 IU/L). A diagnosis of symptomatic fetal CMV infection was made. Immediate delivery was considered to be contraindicated because of the poor prognosis of neonatal care at this gestational age.[1,2] Conversely, no natural improvement in fetal status was expected because maternal serum CMV-specific IgG were insufficiently high to produce anti-viral immune transfer via placenta (Table 1).

With informed choice, fetal ascites was extracted and CMV high titer gamma globulin, Venoglobulin-IH (polyethyleneglycol treated immunoglobulin; CMV IgG 258.0 of EIA cutoff <2.0, × 199 in the neutraliation test, Benesis, Japan), was injected into the fetal abdominal cavity 2.5 g/fetal body (at most 2 g/estimated fetal weight in kg) using a 23-gauge needle under colour Doppler ultrasound guidance. Every two weeks, three times injection was performed in series. The fetal haemoglobin rose to 12.0 g/dL at 32 weeks and to 12.6 g/dL at 34 weeks of gestation. Fetal growth restriction was observed at presentation but the growth rate returned to normal after the initial treatment. Fetal ascites ceased to be visible at 34 weeks of gestation. Maternal serum CMV-DNA disappeared at 32 weeks of gestation without quantitative alteration of serum IgG and IgM. CMV-DNA in the fetal ascites diminished to undetectable level at 34 weeks of gestation, whereas that in amniotic fluid remained high at 7.6×10^6 to 9.3×10^7 copies/mL until delivery (Table 1).

A 2084 g girl was born by elective section at 36 weeks of gestation following the onset of labour with a flexed breech presentation. Mild villositis with CMV inclusion bodies in the placenta was reported pathologically. CMV-DNA was not detected in the newborn serum and urine. Brain CT scan on day four was reported as normal. Whereas auditory brain reaction on day five predicted slight hearing disturbance in the right side. The newborn was healthy and was hospitalised in our regular newborn care unit for two weeks. At age 24 months, she had a compensating hearing disorder of the right side, but other aspects of her neurological, physical and mental development were normal.

Discussion

Cytomegalovirus is a member of the herpes family of viruses and causes a number of infection syndromes in humans. This includes the classic TORCH syndrome, consisting of hepatosplenomegaly, microcephaly, hyperbilirubinaemia, petechiae, thrombocytopenia, hydrops and intrauterine growth restriction. In symptomatic congenital CMV-infected fetus, mortality may be as high as 20–30%, with 90% of survivors suffering late complication.[1,2] CMV is the most common cause of congenital sensorineural hearing loss.[3] Prenatal diagnosis of CMV-infected fetus remains problematical because of a possible recurrent infection during pregnancy including reactivation of the women's own strain of CMV acquired previously, possible reinfection with a new strain of virus,[4] lack of fetal CMV seropositivity for IgM in culture positive fetuses or failure of the fetus to sustain the IgM response. Ultrasonographic demonstration of significant fetal abnormalities

Department of Obstetrics and Gynaecology, National Defense Medical College, Tokorozawa, Saitama, Japan

Correspondence: Dr H. Matsuda, Department of Obstetrics and Gynaecology, National Defense Medical College, 3-2 Namiki, Tokorozawa, Saitama, 359-1513 Japan.

Table 1. Fetal therapy and quantative analysis of CMV-DNA, IgG and IgM.

	29 weeks 4 days	30 weeks 3 days	31 weeks 4 days	32 weeks 3 days	33 weeks 4 days	34 weeks 3 days	35 weeks 4 days
γ-Globulin injection into fetal abdominal cavity (g)		2.5		2.5		2.5	
Maternal serum CMV-DNA (copy/mL)	180.0	54.0	<20	33.0	<20	<20	<20
Amniotic fluid CMV-DNA (million copies/mL)	7.6		67.0	27.0	80.0	93.0	53.0
Fetal ascites CMV-DNA (thousand copies/mL)	23.0		2.0	0.15	0.12	<0.1	<0.1
Umbilical vein serum CMV-DNA (copy/mL)						<20	
Maternal serum CMV-IgG (EIA cutoff: <2.0)	16.0	15.0	17.0	18.0	23.0	15.0	17.0
Maternal serum CMV-IgM (EIA cutoff: <0.8)	1.84	1.80	1.58	1.72	1.77	1.44	1.55
Umbilical vein serum CMV-IgG (EIA cutoff: <2.0)		2.3		8.4		36.0	

in appropriate clinical circumstances, isolation of the virus or DNA from fluid collected by amniocentesis and haematologic, viral or serological information from fetal blood collected by cordocentesis are all methods for antenatal diagnosis.[5,6] Usually, detected CMV-DNA in amniotic fluid reveals a history of fetal viremia, but it does not directly demonstrate the current fetal condition. An effective fetal therapy remains yet to be found.

Ganciclovir administration into the umbilical vein and anti-CMV IgG injections into the fetal abdominal cavity have been reported but the evaluation of the prognosis is not well established.[7,8] In this case, immunoglobulin was selected over ganciclovir because its administration is safer.[7] Fetal administration was considered preferable to maternal administration because the appropriate dose to reach the fetus via the placenta was difficult to estimate and it would also be expensive. Intravascular administration at the time of percutaneous umbilical blood sampling was also abandoned because its safety for the fetal circulation is not yet proven. Direct intraperitoneal administration was desirable because immunoglobulin would not be diluted by fetoplacental circulation and maternal circulation, and it would minimise the influence of the administered volume of immunoglobulin in the fetal circulation. The dose of immunoglobulin was determined referring to an earlier report.[8]

We conclude that an anti-CMV IgG injection into the fetal abdominal cavity is clinically useful. Our data suggest that, after treatment, CMV-DNA in the amniotic fluid was produced in the infected placenta and the amniotic membrane.

References

1. Stagno S, Whitely RJ. Herpesvirus infections of pregnancy. Part I: Cytomegalovirus and Epstein–Barr virus infections. *N Engl J Med* 1985;**313**:1270–1274.
2. Demmler GJ. Infectious Disease Society of America and Center for Disease Control summary of a workshop on surveillance for congenital cytomegalovirus disease. *Rev Infect Dis* 1991;**13**:315–329.
3. Hicks T, Fowler K, Richardson M, Dahle A, Adams L, Pass R. Congenital cytomegalovirus infection and neonatal auditory screening. *J Pediatr* 1993;**123**:779–782.
4. Boppana SB, Rivera LB, Fowler KB, Mach M, Britt WJ. Intrauterine transmission of cytomegalovirus to infants of women with preconceptional immunity. *N Engl J Med* 2001;**344**:1366–1371.
5. Grose C, Weiner CP. Prenatal diagnosis of congenital cytomegalovirus infection: two decades later. *Am J Obstet Gynecol* 1990;**163**:447–450.
6. Guerra B, Lazzarotto T, Quarta S, et al. Prenatal diagnosis of symptomatic congenital cytomegalovirus infection. *Am J Obstet Gynecol* 2000;**183**(2):476–482.
7. Revello MG, Percivalle E, Baldanti F, et al. Prenatal treatment of congenital human cytomegalovirus infection by fetal intravascular administration of ganciclovir. *Clin Diagn Virol* 1993;**1**:61–67.
8. Negishi H, Yamada H, Hirayama E, et al. Intraperitoneal administration of cytomegalovirus hyperimmunoglobulin to cytomegalovirus-infected fetus. *J Perinatol* 1998;**18**(6):466–469.

Accepted 28 January 2004

J. Perinat. Med. 33 (2005) 561–563 • Copyright © by Walter de Gruyter • Berlin • New York. DOI 10.1515/JPM.2005.100

Short communication

Intrauterine therapy for parvovirus B19 infected symptomatic fetus using B19 IgG-rich high titer gammaglobulin

Hideo Matsuda*, Kenichiro Sakaguchi, Tomoko Shibasaki, Hironori Takahashi, Yuichi Kawakami and Kenichi Furuya

Department of Obstetrics and Gynecology, National Defense Medical College, Japan

Abstract

Parvovirus B19-infected hydrops fetalis was treated using gammaglobulin injection into the peritoneal cavity (GIFPeC) with B19-IgG-rich immunoglobulin. Fetal anemia and hydrops resolved, and B19-DNA in fetal ascites decreased despite no change in maternal B19-IgG or B19-DNA. Gammaglobulin injection into the peritoneal cavity is thus useful for treating hydrops fetalis while avoiding intrauterine blood-transfusion risks.

Keywords: Fetal therapy; gammaglobulin; gammaglobulin injection into fetal peritoneal cavity; parvovirus; pregnancy.

Background

Parvovirus B19-infected hydrops fetalis is known to be fatal in approximately 30% of cases. Conventionally, intrauterine blood transfusion has been used to treat infections occurring around 20 weeks' gestation, the period during which prognosis is regarded as being particularly poor. Although effective, intrauterine blood transfusion poses various problems of technical nature, but also involves risk to the fetus, such as a 6% fetal mortality rate, infection from blood transfusion, and low oxygen transport capacity related to the transfused adult hemoglobin. In the present case, we were able to successfully treat a B19-infected symptomatic fetus with severe anemia without resorting to intrauterine blood transfusion by performing gammaglobulin injection into the peritoneal cavity (GIFPeC).

*Corresponding author:
Hideo Matsuda, MD
Department of Obstetrics and Gynecology
National Defense Medical College
3-2 Namiki
Tokorozawa
Saitama Prefecture
Japan 359-1513
Tel.: 81-42-995-1687
Fax: 81-42-996-5213
E-mail: hmatsuda@ndmc.ac.jp

Case

In May 2004, a 37-year-old woman, gravida 2 para 1, was referred at 20 weeks gestation with fetal hydrops. Three weeks previously she had experienced flu-like symptoms following a diagnosis on her and her 8-year-old daughter of erythema infectiosum. The patient had slight dyspnea and pleural effusion revealed by chest radiology. No blood group antibodies were detected, but fetal ascites, skin edema, pericardial effusion, and cardiomegaly were observed. Cyclic estimation of maternal serum B19-specific IgM and IgG EIA (enzyme immunoassay) suggested a primary B19 infection. Maternal serum, amnion, and fetal ascites tested positive for parvovirus B19-DNA with quantitative real-time polymerase chain reaction (PCR). Ultrasound and magnetic resonance scans did not detect organic fetal anomalies. Doppler ultrasound showed fetal anemia (middle cerebral artery peak systolic velocity (MCAPSV): 0.62 m/s). Based on the patient's symptoms and the above test results, a diagnosis of parvovirus B19-infected hydrops fetalis was made (Table 1).

Methods

With the patient's informed consent, it was decided to perform gammaglobulin injection into the peritoneal cavity (GIFPeC) using B19-IgG-rich immunoglobulin. The National Defense Medical College Hospital, Institutional Review Board approved this treatment.

Fetal ascites fluid was extracted and 0.8 g (approximately 2 g/kg) of parvovirus B19 high titer gammaglobulin (26.2; EIA cut-off: 0.80, Benesis, Japan) injected into the fetal abdominal cavity using a 25-gauge needle (Hanaco Medical, Japan) under color-Doppler-ultrasound guidance. Injections were performed twice, at 21 and 22 weeks duration, at an interval of eight days.

Results

Fetal ascites and pericardial effusion clearly decreased within 5 days and had completely disappeared by

Table 1 Fetal therapy and quantative analysis of B19-DNA, IgG, IgM, and fetal MCA-PSV.

	21w3d	21w4d	22w4d	23w0d	23w3d	28w4d	34w3d	37w2d (delivery)
G-globulin[a] injection into fetal abdominal cavity (g)	0.81		0.81					
Maternal serum B19-DNA (thousand copies/mL)	36.1		34.0		26.0	1.6	0.3	<0.1
Maternal serum B19-IgG (EIA cut off: <0.8)	9.64		9.71		11.67	10.27	8.73	7.10
Maternal serum B19-IgM (EIA cut off: <0.8)	8.87		6.47		5.79	3.52	2.26	1.98
Amniotic fluid B19-DNA (thousand copies/mL)	5700.0				4400.0	45.0	2.70	0.25
Amniotic fluid B19-IgG (EIA cut off: <0.8)	3.94					2.23	1.26	1.29
Fetal ascites B19-DNA (thousand copies/mL)	1000.0		57.0		ascites (-)			
Fetal MCAPSV (m/s)[b]	0.62	0.57	0.40	0.22	0.22	0.35	0.51	
Umbilical vein serum B19-IgG (EIA cut off: <0.8)								7.6
Umbilical vein serum B19-DNA (copy/mL)								<0.1

[a]B19-IgG in g-globulin: 26.7 (EIA cut off: <0.8); [b]MCAPSV: Mean cerebral artery peak systolic velocity

22 weeks gestation, as had maternal dyspnea and pleural effusion. Fetal MCAPSV improved rapidly: 0.57 m/s at 1 day, 0.40 m/s at 7 days, and 0.22 m/s at 11 days after primary injection. Thus, fetal anemia and hydrops improved simultaneously. Furthermore, despite no significant change in either maternal B19-IgG or maternal serum B19-DNA, B19-DNA in the fetal ascites fluid decreased significantly, from 1.0×10^6 copies/mL to 5.7×10^4 copies/mL, by 7 days after treatment.

The patient was released from hospital after two weeks. She was readmitted at 38 weeks gestation for an elective cesarean section and a healthy boy (Apgar score: 8/9) weighing 2,308 g was delivered. No B19-DNA was detected in the newborn's serum, and there was no cardiac dysfunction.

Discussion

Parvovirus B19 is not only cytotoxic for fetal red blood cell precursors (leading to fetal anemia) [1], but also stimulates a cellular process initiating cellular apoptosis (parvovirus myocarditis) [6]. The possibility of B19 infection in pregnancy is estimated to be 3.5% [9] and 8.3–20.0% of infected fetuses die *in utero* [7]. Risk is highest in the first trimester, with 10.0–23.1% spontaneous abortions or fetal deaths prior to 20 weeks gestation [7, 9]. Hydrops fetalis resulting from fetal anemia can lead extremely rapidly to death [4], but resolves spontaneously in 34% of cases [3, 8].

Doppler assessment of fetal MCAPSV is an accurate tool for determining fetal anemia and is a non-invasive alternative to cordocentesis [2] and was used to gauge treatment efficacy in the present study because of the possible risks of cordocentesis. However, fetal treatment without cordocentesis is not yet established. One case of a parvovirus B19-infected woman being treated intravenously with gammaglobulin during pregnancy has been documented [10], but this method is not cost-effective. Rodis et al. [8] have shown intrauterine transfusion to be an effective treatment, reporting recovery in 29% of cases after intrauterine transfusion versus death in 30% without intervention. However, they also reported death after transfusion in as many as 6% of case. Since this report does not record parvovirus B19 antibody levels in the transfused blood, it is unclear whether the recoveries were due to the transfusion of adult blood or to B19 antibodies in the transfused blood.

Gammaglobulin injection into the peritoneal cavity (GIFPeC) has already been used to treat a cytomegalovirus-infected symptomatic fetus [5], and is a comparatively safe treatment method in that it avoids cordocentesis. Peritoneal injection avoids direct preload on fetal circulation during the procedure and enables administration of higher quantities. As gammaglobulin is a heated blood product, the risk of infection is lower than that of blood transfusion. Furthermore, since package inserts list viral antibody levels, it is possible to order and use vials containing high levels of antibodies to specific viruses. Such factors, combined with the results obtained in this case, indicate that gammaglobulin injection into the peritoneal cavity (GIFPeC) may be a clinically useful therapy for parvovirus B19-infected hydrops fetalis.

References

[1] Brown KE, SM Anderson, NS Young: Erythrocyte P antigen: Cellular receptor for B19. Science 262 (1993) 114

[2] Cosmi E, G Mari, LD Chiaie, et al.: Noninvasive diagnosis by Doppler ultrasonography of fetal anemia resulting from parvovirus infection. Am J Obstet Gynecol 187 (2002) 1290
[3] Fairley C, J Smoleniec, O Caul, E Miller: Observational study of effect of intrauterine transfusions on outcome of fetal hydrops after parvovirus B19 infection. Lancet 346 (1995) 1335
[4] Jordan J: Identification of human parvovirus B19 infection in idiopathic nonimmune hydrops fetalis. Am J Obstet Gynecol 16 (1996) 342
[5] Matsuda H, Y Kawakami, K Furuya, Y Kikuchi: Intrauterine therapy for cytomegalovirus infected symptomatic fetus. BJOG 111 (2004) 756
[6] More AL, DJ Ferguson, KA Flemming: Ultrastructural features of fetal erythroid precursors infected with parvovirus B-19 *in-vitro*: Evidence of cell death by apoptosis. J Pathol 169 (1993) 213
[7] Public Health Laboratory Service Working Party on Fifth Disease. Prospective study of human parvovirus (B19) infection in pregnancy. BMJ 300 (1990) 1166
[8] Rodis JF, AF Borgida, M Wilson, et al.: Management of parvovirus infection in pregnancy and outcomes of hydrops: A survey of members of the Society of Perinatal Obstetricians. Am J Obstet Gynecol 179 (1998) 985
[9] Rodis JF, DL Quinn, WJ Garry, et al.: Management and outcomes of pregnancies complicated by Human B19 parvovirus infection: A prospective study. Am J Obstet Gynecol 163 (1990) 1168
[10] Selbing A, A Josefuson, LO Dahle, R Lindgren: Parvovirus B19 infection during pregnancy treated with high-dose intravenous gammaglobulin. Lancet 345 (1995) 660

Received July 7, 2005. Accepted July 22, 2005.